

Fermi-liquid behavior in the electrical resistivity of K_3C_{60} and Rb_3C_{60}

T. T. M. Palstra, A. F. Hebard, R. C. Haddon, and P. B. Littlewood

AT&T Bell Laboratories, Murray Hill, New Jersey 07974

(Received 18 March 1994)

We report on the electrical resistivity of K_3C_{60} and Rb_3C_{60} thin films. These films, grown at elevated temperatures, are highly textured and consist of large single-crystal grains. The films exhibit metallic behavior up to 500 K, with residual resistivities of 1.2 m Ω cm. The low-temperature (T) resistivity exhibits a T^2 dependence. We suggest that it is dominated by electron-electron interactions, and we find quantitative agreement not only with estimates based on the electron density and the bandwidth, but also with other narrow band systems. The electron-phonon interactions only become important for the resistivity above room temperature, because these phonons correspond to high-frequency vibrations of the C_{60} molecule. Nevertheless, virtual excitations of these same high-energy phonons are responsible for the superconductivity. Using similar criteria of conventional organic superconductors, we find that these materials are dominated at all temperatures by electron-phonon interactions.

Electrical resistivity measurements have provided a wealth of information on the conduction mechanism and Fermi-surface properties of organic conductors.¹⁻³ From the temperature and magnetic-field dependence of the resistivity the scattering mechanisms can be derived, and for clean samples the Fermi surface can be mapped. For alkali-doped C_{60} the situation seems to be more complicated and even for "optimally" doped samples with stoichiometry near A_3C_{60} (A = alkali metal) the resistivity is only slightly smaller than the value at the metal-to-insulator boundary.⁴⁻⁸ These high resistivities have thus far precluded transport studies of Fermi-surface properties and, moreover, it is not clear what mechanisms are responsible for limiting the conductivity. Our interest in the conductivity stems from the fact that the inelastic-scattering mechanisms causing electrical resistivity are usually identical to the interactions leading to superconductivity.

To study intrinsic electrical transport properties of doped C_{60} , we have made metallic thin films, exhibiting normal-state resistivities that are at least as good as reported for the best single crystals.⁶ Using thin films we have excellent control of the geometry and obtain homogeneous doping through the film, avoiding problems usual for single crystals. Our earlier K_3C_{60} films exhibited granular behavior, and the grain size was found to determine the electrical transport behavior. Therefore, we modified our growth procedure⁸ to one that yields large grains and metallic resistivities with a typical residual resistivity ratio of $\rho(RT)/\rho(T_c) \sim 2$. Surprisingly, these metallic films have a resistivity at room temperature of ~ 2 m Ω cm, which is similar to the values of the granular films⁵ which exhibited a negative temperature coefficient $d\rho/dT$. However, near T_c the resistivities of these two types of films are different by a factor of 3, which is reflected in a smaller value of the upper critical field slope.

In this article we will discuss the strong electron scattering in A_3C_{60} . We argue that the low-temperature resistivity is dominated by electron-electron interactions,

and find quantitative agreement not only with estimates based on the electron density and the band width, but also with other narrow-band systems. The electron-phonon interactions become only important for the resistivity above room temperature. The high superconducting transition temperatures are caused by virtual excitations of high-energy phonons, which are not thermally excited at low temperature.

The films were vacuum sublimed in a tube furnace. The C_{60} powder source was in the center of the furnace at $\sim 400^\circ\text{C}$, and the glass substrate near the end of the furnace at $\sim 200^\circ\text{C}$. In this way a deposition rate was obtained of about 500 $\text{\AA}/\text{h}$. After deposition the films were mounted in a glass tube with electrical feedthroughs. After evacuating the tube the minimum resistivity was attained by repetitive doping and anneal cycles at 150°C .

The films were examined with x rays. The linewidths are resolution limited and show that the films are highly textured along the (1 1 1) planes.⁸ The electrical resistivity was measured using a Linear Research resistance bridge (LR400), and always found to be Ohmic. Measurements below room temperature (RT) were performed in a liquid-helium dewar containing a 15 T superconducting magnet, and above RT in a tube furnace. The temperature was monitored with calibrated carbon-glass and platinum resistance thermometers, mounted outside the glass tube, which was placed in an isothermal brass can. Since the thermal response of the sample was very slow, the temperature was changed very slowly by a heater mounted on the brass can.

In Fig. 1 we show the electrical resistivity of K_3C_{60} and Rb_3C_{60} thin films, heating the samples from 4 to 500 K. We studied five K_3C_{60} films and three Rb_3C_{60} films. The typical resistivity at RT is 2 m Ω cm. Cooling down to the superconducting transition results in residual resistivity ratios between 1 and 2. Our best films have a residual resistivity of 1.2 m Ω cm for both K_3C_{60} and Rb_3C_{60} . We note that due to the slow thermal response of our system, the samples were quickly cooled to liquid helium and then slowly heated to RT, while recording the resis-

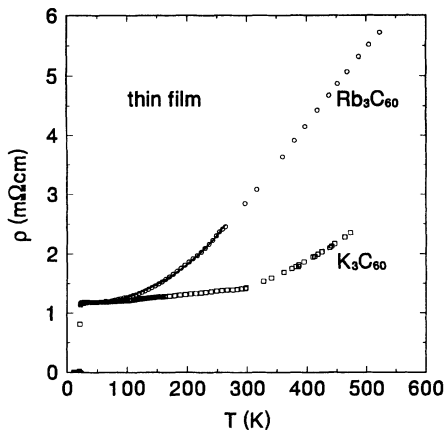


FIG. 1. Temperature dependence of the electrical resistivity of K_3C_{60} and Rb_3C_{60} thin films between 4 and 500 K. The solid line through the data of Rb_3C_{60} between 50 and 250 K is a fit including both electron-electron and electron-phonon interactions.

tivity. When temperature cycling the films, the initial RT value was never reproduced. Our measurements showed that the resistivity exhibits wide hysteresis loops. The hysteresis is only observed in the first cooling to 4 K, and subsequent temperature cycling between 4 K and RT yields reversible behavior, shown in Fig. 1. Heating the samples above RT can recover the original state, depending on the highest temperature and the time at elevated temperatures.

We show in Fig. 2 the behavior near the superconducting transition of K_3C_{60} and Rb_3C_{60} films. The transition is very sharp with the 10–90% width of the transition ~ 1 K. Applying a field up to 12.5 T shifts the midpoint

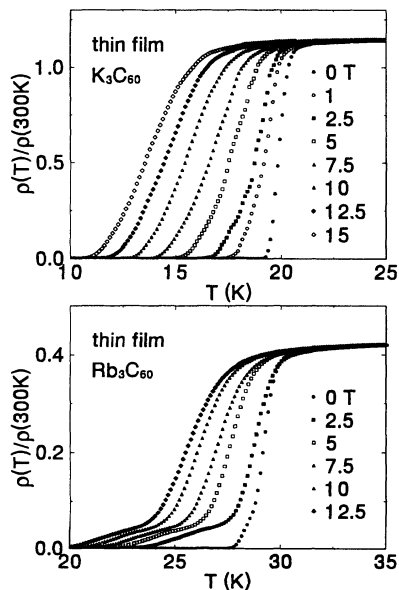


FIG. 2. Temperature dependence of the electrical resistivity of K_3C_{60} and Rb_3C_{60} near the superconducting transition in magnetic fields of 0, 1, 2.5, 5, 7.5, 10, 12.5, and 15 T. The magnetic field was oriented perpendicular to the current direction.

of the transition at a rate of 2.65 T/K for K_3C_{60} and 3.5 T/K for Rb_3C_{60} . In this Rb_3C_{60} film evidence for weak links is seen in the resistance “foot” of the transition.⁹

In discussing these materials we will focus on two aspects of our measurements, namely the magnitude and the temperature dependence of the electrical resistivity. We will use measurements on other conductors as a reference for our observations. The residual resistivity of 1.2 m Ω cm for the present films is at least as good as reported for the best single crystals.⁶ Slightly smaller values of the resistivity were inferred from reflectivity measurements,¹⁰ but this difference can be associated with the nonspecular surface of the powder samples, and the resulting error in the determination of the absolute value of the conductivity.

The question can be raised whether the resistivity is intrinsic or due to geometric factors which give rise to a tortuous current path. From the upper critical field slopes we derive Ginzburg-Landau coherence lengths of 31 and 22 Å for K_3C_{60} and Rb_3C_{60} , respectively. Since the Pippard coherence length can be estimated from the band structure to be $\xi_0 \approx 140$ Å, we are in the dirty limit. In this case the upper critical field slope is given by¹¹

$$-dH_{c2}/dT|_{T=T_c} = 4780\gamma\rho_0 \quad (1)$$

with γ the renormalized linear specific-heat coefficient and ρ_0 the residual resistivity. Thus, we can use the upper critical field slope as a direct measure of the intrinsic value of the resistivity on the length scale of the pair-breaking process ($\sim \xi$). Using appropriate estimates for γ (see below), we find that the measured values of the resistivities are indeed intrinsic and thus relevant to the pair-breaking process, and also for superconductivity.

It is of paramount importance to establish whether the low-temperature conductivity in A_3C_{60} is in keeping with a Fermi-liquid description. A resistivity of 1 m Ω cm is for most materials above the Mott limit, and would render them insulating. Therefore, we will first determine the Mott limit for this material. For a Fermi-liquid description to be appropriate, it requires that $k_F l > 1/2\pi$, with k_F the Fermi wave vector, and l the mean free path at zero temperature averaged over the Fermi surface.¹² We establish $k_F l$ by using the general relation between the conductivity and the Fermi-surface area S_F , assuming an isotropic mean free path¹²

$$\sigma = \frac{e^2}{\hbar} \frac{1}{12\pi^3} (S_F l). \quad (2)$$

Although the Fermi surface is not known in detail, one may crudely estimate $k_F l$ in two limiting cases. One is the single noninteracting band with three carriers per C_{60} molecule. Combined with the experimental residual resistivity of 1.2 m Ω cm, this yields $k_F l \approx 2.5$ as an upper bound for the mean free path at low temperatures. If there were three degenerate parabolic bands (derived from the t_{1u} orbitals), we would obtain $k_F l \approx 1$. In either case the conductivity is somewhat larger than the characteristic conductivity scale,¹²

$$\sigma_{\text{mott}} = 0.01 e^2 k_F / \hbar, \quad (3)$$

which we estimate to be in the range $0.5\text{--}0.7\text{ (m}\Omega\text{ cm)}^{-1}$ depending on the assumed k_F . Thus a Fermi-liquid description of the metallic state is appropriate. The Mott limit for A_3C_{60} is smaller than in regular metals because of the low conduction-electron density.

In the three-dimensional Bloch-Grüneisen model, the acoustic phonons give rise to a T^3 temperature dependence, whereas electron-electron Umklapp scattering results in T^2 behavior. Our data on Rb_3C_{60} exhibit a temperature dependence that can be accurately fitted between 50 and 250 K with $A^*T^2 + B^*T^3$, with a coefficient $A = 10^{-2}\text{ }\mu\Omega\text{ cm/K}^2$ and $B = 3.6 \times 10^{-5}\text{ }\mu\Omega\text{ cm/K}^3$, as shown in Fig. 3. We can make theoretical estimates of both parameters to see what values can be expected for A_3C_{60} . The electronic T^2 coefficient A can be estimated from

$$A \sim \frac{1}{\omega_p^2 \tau_0} \frac{1}{T_F^2} \quad (4)$$

with τ_0^{-1} the bare scattering rate, and ω_p the plasma frequency. ω_p depends only on the electron density and is roughly 1 eV.¹³ The scattering rate can be estimated from Coulomb interactions of an electron gas with an average separation between the electrons of a_L : $\hbar/\tau_0 \sim e^2/a_L = (a_0/a_L) \times 27\text{ eV}$, with a_0 the Bohr radius. This yields $\tau_0 \sim 1\text{ eV}$. Using a Fermi temperature $T_F \sim 1500\text{--}2000\text{ K}$, based on susceptibility measurements¹⁴ we find that $A \sim 1\text{--}2 \times 10^{-2}\text{ }\mu\Omega\text{ cm}$. Thus the magnitude of the T^2 term is consistent with a simple estimate of the electronic scattering.

The electron-phonon contribution to the resistivity was calculated, and estimated to be $69\text{ }\mu\Omega\text{ cm}$ at 260 K.¹⁵ Other calculations obtained $160\text{ }\mu\Omega\text{ cm}$ at 260 K.⁶ Both estimates are an order of magnitude smaller than the experimentally observed increase between T_c and 260 K, supporting our view that the low-temperature resistivity is dominated by electron-electron interactions. Conversely, if one interprets the resistivity with electron-phonon scattering, unreasonably large values of the coupling con-

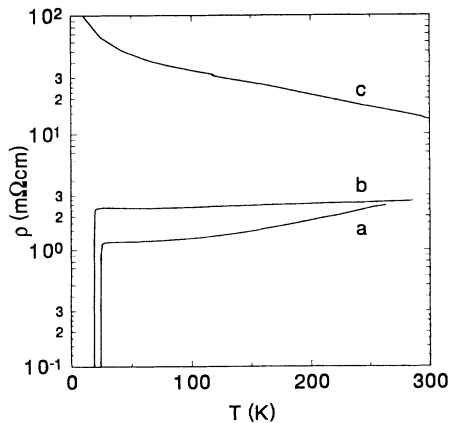


FIG. 3. Temperature dependence of the electrical resistivity of (a) crystalline Rb_3C_{60} , (b) granular K_3C_{60} , and (c) underdoped granular K_xC_{60} ($x < 3$) thin films.

stant $\lambda > 1$ are required.⁸ However, it is thought that the pairing mechanism for superconductivity is due to electron-phonon interactions,¹⁶ and usually, the interactions leading to resistivity are identical to those leading to superconductivity. However, in A_3C_{60} the phonons with a large coupling to the electrons have been attributed to two optical modes with energies above 1000 K.¹⁶ These high-frequency phonons mediate superconductivity via virtual excitations, but these vibrational states will not be appreciably populated under the conditions of our experiment. Of course, the high-frequency virtual phonons can induce changes in the magnitude of the T^2 resistivity by moderating the effective $el-el$ interaction.¹⁷

Equation (4) was confirmed for many materials¹⁸ by relating the resistivity coefficient A to γ , the linear specific-heat coefficient, which is linear with T_F^{-1} (see Fig. 4). All narrow-band systems fall on one line with slope 2. The transition metals have the same slope but a different proportionality factor. For A_3C_{60} we can estimate γ from the specific-heat jump at T_c ,¹⁴ which results in a value of 48 mJ/mol K^2 . This puts Rb_3C_{60} on the line for narrow-band systems. Of course, the origin of the narrow band is different for the various materials, arising here from the small wave-function overlap. Using literature values,¹⁹ we note that intercalated graphite KC_8 also falls on this line, even though γ is an order of magnitude smaller. KC_8 is similar to A_3C_{60} in that superconductivity is mediated by high-frequency optical phonons. However, it should be pointed out that in two-dimensional materials the resistivity due to acoustic phonons also gives rise to a T^2 dependence. In KC_8 the resistivity can be totally accounted for by $el-el$ interactions, given its value of γ . For other two-dimensional organic superconductors,²⁰ the ET-salts, the resistivity coefficient A is far larger than expected from the Fermi temperature, and

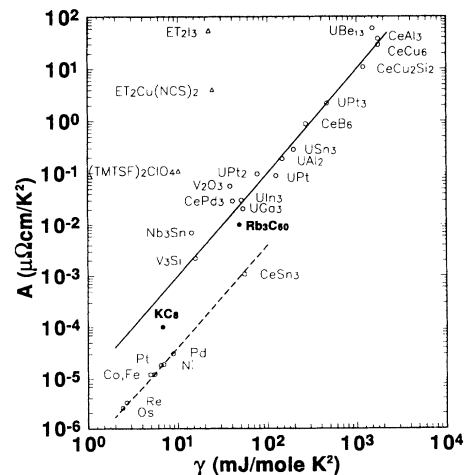


FIG. 4. Resistivity coefficient A vs linear specific-heat coefficient γ for wide- and narrow-band conductors. The line through the heavy fermion compounds and the $A15$ compounds corresponds to $A/\gamma^2 = 1 \times 10^{-5}$, and includes Rb_3C_{60} and KC_8 . The line through the transition metals corresponds to $A/\gamma^2 = 0.4 \times 10^{-6}$. The traditional organic superconductors have much larger ratios A/γ^2 .

the resistivity seems to be dominated by phonons. This strongly suggests that superconductivity in the conventional organic conductors is also mediated by electron-phonon interactions.

Thus we suggest the following picture for the temperature-dependent transport properties. Usually, in charge-transfer conductors the electrical conductivity is thought to be dominated by the charge-transfer integral between adjacent molecules, resulting in a bandwidth that should be compared with the on-site Coulomb repulsion. However if we take the Fermi-surface area for K_3C_{60} ($2.4 \times 10^{16} \text{ cm}^{-2}$) from the band-structure calculation by Erwin²¹ and solve Eq. (1), we obtain a mean free path, $l = 5 \text{ \AA}$. Thus the mean free path is smaller than the size of a C_{60} molecule and the temperature-dependent scattering is taking place on the C_{60} molecule.²² If we take the radius of the C_{60} molecule as 3.5 \AA then the circumference of the molecule is 22 \AA , this allows the three conduction electrons to be placed on the molecule with a

7-\AA separation, in good agreement with the mean-free-path estimate. This crude model has analogy with a previous picture developed to explain the delayed ionization of C_{60} in terms of the annihilation of multiple excitons which migrate over the surface of the molecule.²³

In conclusion, we have studied crystalline films of K_3C_{60} and Rb_3C_{60} . The films exhibit sharp superconducting transitions and metallic behavior up to 500 K, with a residual resistivity of $1.2 \text{ m}\Omega \text{ cm}$. The films are in the dirty limit with mean free paths comparable to the size of a C_{60} molecule. The resistivity is smaller than the Mott limit, and thus a Fermi-liquid description is appropriate. The parameters describing the transport data are consistent with an electron-electron scattering mechanism, which is large because the bandwidth is narrow.

We would like to acknowledge stimulating discussions with Y. Iwasa, A. Millis, A. P. Ramirez, B. S. Shastry, G. A. Thomas, C. M. Varma, and J. Zaanen.

¹T. Ishiguro and K. Yamaji, *Organic Superconductors* (Springer, Berlin, 1990).

²*The Physics and Chemistry of Organic Superconductors*, edited by G. Saito and S. Kagoshima (Springer, Berlin, 1990).

³*Graphite Intercalation Compounds*, edited by H. Zabel, and S. A. Solin (Springer, Berlin, 1992).

⁴G. P. Kochanski, A. F. Hebard, R. C. Haddon, and A. T. Fiory, *Science* **255**, 184 (1992).

⁵T. T. M. Palstra, R. C. Haddon, A. F. Hebard, and J. Zaanen, *Phys. Rev. Lett.* **68**, 1054 (1992).

⁶V. H. Crespi, J. G. Hou, X.-D. Xiang, M. L. Cohen, and A. Zettl, *Phys. Rev. B* **45**, 2064 (1992); X.-D. Xiang, J. G. Hou, G. Briceno, W. A. Vareka, R. Mostovoy, A. Zettl, V. H. Crespi, and M. L. Cohen, *Science* **256**, 1190 (1992).

⁷Z. H. Wang, A. W. P. Fung, G. Dresselhaus, M. S. Dresselhaus, K. A. Wang, P. Zhou, and P. C. Eklund, *Phys. Rev. B* **47**, 15 354 (1993).

⁸A. F. Hebard, T. T. M. Palstra, R. C. Haddon, and R. M. Fleming, *Phys. Rev. B* **48**, 9945 (1993).

⁹S. H. Glarum, S. J. Duclos, and R. C. Haddon, *J. Am. Chem. Soc.* **114**, 1996 (1992).

¹⁰L. Degiorgi, P. Wachter, G. Gruener, S.-M. Huang, J. Wiley, and R. B. Kaner, *Phys. Rev. Lett.* **69**, 2987 (1992).

¹¹T. P. Orlando, E. J. McNiff, S. Foner, and M. R. Beasley, *Phys. Rev. B* **19**, 4545 (1979).

¹²N. F. Mott, *Metal-Insulator Transition* (Taylor and Francis, London, 1990), p. 28.

¹³Y. Iwasa, K. Tanaka, T. Yasuda, and T. Koda, *Phys. Rev. Lett.* **69**, 2284 (1992).

¹⁴A. P. Ramirez, M. J. Rosseinsky, D. W. Murphy, and R. C.

Haddon, *Phys. Rev. Lett.* **69**, 1687 (1992).

¹⁵V. P. Antropov, O. Gunnarsson, and A. I. Liechtenstein, *Phys. Rev. B* **48**, 7651 (1993).

¹⁶C. M. Varma, K. Raghavachari, and J. Zaanen, *Science* **254**, 989 (1991); M. Schluter, M. Lannoo, M. Needles, G. A. Baraff, D. Tomanek, *Phys. Rev. Lett.* **68**, 526 (1992); R. A. Jishi and M. S. Dresselhaus, *Phys. Rev. B* **45**, 2597 (1992).

¹⁷A. Millis (private communication) and L. N. Bulaevski, *Adv. Phys.* **37**, 443 (1988).

¹⁸K. Miyake, T. Matsuura, and C. M. Varma, *Solid State Commun.* **71**, 1149 (1989), and references therein.

¹⁹M. S. Dresselhaus and G. Dresselhaus, *Adv. Phys.* **30**, 139 (1981).

²⁰K. Murata, Y. Honda, H. Anzai, M. Tokumoto, K. Takahashi, N. Kinoshita, and T. Ishiguro, *Synth. Met.* **27**, A263 (1989); S. Ikihata, T. Morimoto, H. Suimatsu, and S. Tanuma, *ibid.* **12**, 313 (1985); T. T. M. Palstra (unpublished).

²¹S. C. Erwin and W. E. Pickett, *Science*, **254**, 892 (1991); S. C. Erwin (private communication).

²²Digiorgi *et al.* calculate a much larger mean free path of about 45 \AA , which would become 180 \AA for a more reasonable value for the Fermi velocity. However, their model assumes that less than 1% of the carriers in the t_{1u} band contribute to the dc conductivity. We assume that all carriers of the t_{1u} band contribute to the conductivity. L. Degiorgi, G. Gruener, P. Wachter, S.-M. Huang, J. Wiley, R. L. Whetten, R. B. Kaner, K. Holczer, and F. Diederich, *Phys. Rev. B* **46**, 11 250 (1992).

²³Y. Zhang and M. Stuke, *Phys. Rev. Lett.* **70**, 3231 (1993).